STEM CELLS TRANSLATIONAL MEDICINE®

ENABLING TECHNOLOGIES FOR CELL-BASED CLINICAL TRANSLATION

Quantitative Microplate Assay for Studying Mesenchymal Stromal Cell-Induced Neuropoiesis

IRINA AIZMAN, MICHAEL MCGROGAN, CASEY C. CASE

Key Words. Bone marrow stromal cells • Neural differentiation • Astrocytes • Cytokines • Nestin • Neuron • Oligodendrocytes

SanBio, Inc., Mountain View, California, USA

Correspondence: Irina Aizman, Ph.D., SanBio, 231 South Whisman Road, Mountain View, California 94041-1522, USA. Telephone: 650-625-8965, ext. 52; Fax: 650-625-8969; E-Mail: irina.aizman@san-bio.com

Received September 17, 2012; accepted for publication December 11, 2012; first published online in SCTM *EXPRESS* February 19, 2013.

1066-5099/2013/$20.00/0

http://dx.doi.org/10.5966/sctm.2012-0119

ABSTRACT

Transplanting mesenchymal stromal cells (MSCs) or their derivatives in a neurodegenerative environment is believed to be beneficial because of the trophic support, migratory guidance, and neurogenic stimuli they provide. There is a growing need for in vitro models of mesenchymal-neural cell interactions to enable identification of mediators of the MSC activity and quantitative assessment of neuropoietic potency of MSC preparations. Here, we characterize a microplate-format coculture system in which primary embryonic rat cortex cells are directly cocultured with human MSCs on cell-derived extracellular matrix (ECM) in the absence of exogenous growth factors. In this system, expression levels of the rat neural stem/early progenitor marker nestin, as well as neuronal and astrocytic markers, directly depended on MSC dose, whereas an oligodendrogenic marker exhibited a biphasic MSC-dose response, as measured using species-specific quantitative reverse transcription-polymerase chain reaction in total cell lysates and confirmed using immunostaining. Both neural cell proliferation and differentiation contributed to the MSC-mediated neuropoiesis. ECM's heparan sulfate proteoglycans were essential for the growth of the nestin-positive cell population. Neutralization studies showed that MSC-derived fibroblast growth factor 2 was a major and diffusible inducer of rat nestin, whereas MSC-derived bone morphogenetic proteins (BMPs), particularly, BMP4, were astrogenesis mediators, predominantly acting in a coculture setting. This system enables analysis of multifactorial MSC-neural cell interactions and can be used for elucidating the neuropoietic potency of MSCs and their derivative preparations. STEM CELLS TRANSLATIONAL MEDICINE *2013;2:223–232*

INTRODUCTION

The benefits of transplanting mesenchymal stromal cells (MSCs) or MSC derivatives into the nervous system have been demonstrated in many models of neurodegenerative diseases including stroke, Parkinson's disease, spinal cord injury, multiple sclerosis, and neonatal hypoxic-ischemic brain injury [1–8]. Although the precise mechanisms are not fully understood, the beneficial effects of MSC transplantations are thought to be due to the activation of endogenous regeneration mechanisms in the host neural tissue. These regenerative processes include the enhanced proliferation of endogenous neural stem cells [9–13], as well as the increased survival of newly formed neurons [9–10], gliogenesis [6], and the modulation of inflammatory cytokine production [14]. Transplanted MSCs or their derivatives most likely trigger these processes by secreting diffusible neurotrophic factors and cytokines. MSCs produce a broad range of these factors in culture [15–17], and the spectrum may be modulated by transplantation in neurodegenerative environment [18]. Transplanted cells may also produce locally acting factors, such as extracellular matrix (ECM) molecules and matricellular proteins, which may accumulate and modulate the activity of MSC-derived as well as host tissue-derived neurotrophic factors [19], thereby providing guidance cues and regulating cell recruitment and survival [20, 21].

The effects of MSCs on proliferation and differentiation of neural stem cells into various neural lineages (neuropoiesis) are usually studied in vitro using mitogen-driven neurospheres as a source of neural stem/early precursor cells; subsequently, their differentiation is induced by plating neurospheres on an adhesive substrate and withdrawing the mitogenic growth factors [22–25]. However, cells in neurospheres may not reflect a natural pool of neural precursors because their growth conditions select for responders to nonphysiologically high concentrations of growth factors and unattached growth [26, 27]. Furthermore, induction of neural differentiation through the change of cell attachment status may obscure the effects of test substances (MSCs or their conditioned medium [MSC-CM]).

SB623 cells are produced from MSCs using transient transfection with a vector encoding the human Notch1 intracellular domain (NICD).

SB623 cells are currently in a clinical trial for intracranial treatment of chronic stroke. We have previously shown that ECM produced either by MSCs or by SB623 cells supports the growth and differentiation of rat embryonic cortical cells, with SB623 cell-derived ECM supporting more robust cell growth [28]. In other in vitro models comparing SB623 cells with their parental MSCs, SB623 cells exhibited advantageous immunosuppressive [29] and similar neurotrophic properties [30].

The goal of this study was to develop and validate an in vitro system enabling mechanistic and quantitative analysis of MSC-induced neuropoiesis in a medium-throughput format. The system described here uses a primary rat neural cell population and human MSC "off-the shelf" preparations, which are cocultured at a low plating density on SB623 cell-derived ECM. The ECM substrate appears to be permissive for the growth of cells with different attachment requirements, including neural precursors, neurons, glial cells, and MSCs.

We established the MSC-dose dependence and the time course of accumulation of rat neural differentiation markers in cocultures; we also demonstrated the role of MSC-derived fibroblast growth factor 2 (FGF2) and bone morphogenetic proteins (BMPs) in these processes, where FGF2 and BMP exemplify diffusible and cell/ECM-associated products of MSC activity, correspondingly. The data suggest that the system can be useful for identifying MSC neurogenic and gliogenic factors and for comparing the neuropoietic potency of various MSC preparations.

Materials and Methods

MSC and SB623 Cell Preparations

Our MSC and SB623 cell preparations and their properties were described previously [28]. Briefly, human adult bone marrow aspirates (Lonza, Walkersville, MD, http://www.lonza.com) were grown in α-minimum essential medium (αMEM) (Mediatech Inc., Manassas, VA, http://cellgro.com) supplemented with 10% fetal bovine serum (FBS) (HyClone, Logan, UT, http://www.hyclone.com), 2 mM L-glutamine, and penicillin/streptomycin (both from Invitrogen, Carlsbad, CA, http://www.invitrogen.com). On the second passage, some cells were cryopreserved (MSC preparation) and some cells were plated for the preparation of SB623 cells. For SB623 cell preparation, MSCs were transfected with a pCI-neo expression plasmid encoding the human NICD. The next day, transfected cells were selected for 7 days using G418 (Invitrogen), followed by two passages for culture expansion, harvesting, and cryopreservation. MSCs from seven donors and SB623 cells from five donors were used in this study. For coculture experiments, cells were thawed, washed, and resuspended in a neural growth medium consisting of Neurobasal medium supplemented with B27 and 0.5 mM GlutaMAX (NB/B27/GLX) (all from Invitrogen). For the production of ECM coating or conditioned media, cells were plated in αMEM supplemented with 10% FBS and penicillin/streptomycin (αMEM/FBS/PS).

Plate Coating

For the preparation of wells coated with ECM, SB623 cells were plated at 3×10^4 cells per cm^2 in 96-well plates (Corning Inc., Corning, NY, http://www.corning.com) or on glass coverslips (Fisher Scientific, Pittsburgh, PA, http://www.fisherscientific.com), which were placed into 12-well plates (Corning). After 5 days of culturing, the medium was changed to serum-free and culturing was continued for 2 days followed by cell removal using a modification of the protocol described previously [28]. Briefly, cells were treated with 0.2% Triton X-100 (Sigma-Aldrich, St. Louis, MO, http://www.sigmaaldrich.com) in water at room temperature for 40 minutes; then, cell lysates were aspirated, and a 1:100 solution (vol/vol) of concentrated NH_4OH (Sigma-Aldrich) was added, incubated for 5–7 minutes, and then removed. Afterward, the wells were filled with phosphate-buffered saline (PBS) and incubated for at least 3 hours at room temperature. Wells were either used immediately or stored at 4°C not longer than 3 weeks. In some experiments, ECM was pretreated overnight with Heparinase 1 (Sigma-Aldrich) at the indicated concentrations; the pretreatment was carried out at room temperature, and the wells were washed once.

Ornithine/fibronectin coating (Orn/Fn) was prepared by incubating wells with poly-L-ornithine (Sigma-Aldrich), 15 μg/ml in PBS, overnight at 37°C, then washing wells three times, followed by incubation overnight with PBS at 37°C. Then wells were incubated with bovine fibronectin (Sigma-Aldrich), 1 μg/ml in PBS, for at least 3 hours and washed once before plating cells.

Conditioned Medium (MSC-CM) Preparation

MSCs were plated at 3×10^4 cells per cm^2 and grown in αMEM/FBS/PS for 3–4 days until confluent. The medium was replaced with Neurobasal medium for 1 hour, and then again with Neurobasal medium, half of the volume used for cell growth (for example, 25 ml of Neurobasal medium was conditioned in a T225 flask) for 24 hours. This medium was collected, centrifuged, aliquoted, and stored at −80°C. MSC-CM preparations were supplemented with B27 and 0.5 mM GlutaMAX before use.

Preparation of Rat Embryonic Brain Cortical Cells

Rat embryonic day 18 (E18) brain cortex pairs were purchased from BrainBits (Springfield, IL, http://www.brainbitsllc.com), and a cell suspension was prepared as described previously [28]. Briefly, cortices were incubated with 0.25% trypsin/EDTA (Mediatech) at 37°C for 5–7 minutes and then washed with αMEM containing 10% FBS, and then with PBS. Deoxyribonuclease (DNase) (MP Biomedicals, Solon, OH, http://www.mpbio.com) at 0.25 mg/ml was then added, and the tube was vortexed for 30 seconds. The resulting cell suspension was triturated, washed with PBS, and resuspended in NB/B27/GLX.

Coculture Experiments

Plates coated as described above were prewarmed at 37°C with 50% of final volume of NB/B27/GLX, followed by the addition of MSCs at varying plating densities and neural cells at a constant plating density of 1.5×10^4 cells per cm^2. In some experiments, all ingredients were added to an intermediate plate, mixed, and then distributed to ECM-coated culture plates. For each time point, a separate plate with samples in quadruplicates was used. For the MSC-dose response, MSC plating densities were between 0 and 1.5×10^3 cells per cm^2 (in 96-well plates this corresponded to 0–500 cells per well). For immunostaining, cultures were plated on ECM-coated coverslips in 12-well plates, and MSCs were used at 1.5×10^3 cells per cm^2 unless indicated otherwise.

In experiments comparing the effects of live MSCs to MSC-CM, a cryopreserved aliquot of MSCs was used to generate the MSC-CM prior to an experiment, and another aliquot was used to

generate a corresponding cell suspension. In experiments comparing adherent and nonadherent cell growth, Ultra-Low Attachment (ULA) Costar 96- or 24-well plates (Corning) were used for nonadherent growth. Recombinant FGF2 and epidermal growth factor (EGF) (R&D Systems Inc., Minneapolis, MN, http://www.rndsystems.com, or Peprotech, Rocky Hill, NJ, http://www.peprotech.com) were added at 20 ng/ml each as a positive control to some ULA wells.

Media were not changed during coculture experiments, which typically lasted for 7 days in 96-well format and up to 14 days on coverslips in 12-well plates without signs of culture decline. The cell viability was above 90% at the end of culturing when tested using trypan blue exclusion. For morphological assessments, cocultures were fixed with 4% paraformaldehyde (PFA) (Electron Microscopy Science, Hatfield, PA, http://www.emsdiasum.com/microscopy) and stained with Accustain Hematoxylin Gill#1 and Eosin Y solutions (both from Sigma-Aldrich).

Growth Factor Neutralization Experiments

Effects of neutralizing antibodies in cocultures were tested in the presence of 600 cells per cm^2 MSCs. Anti-FGF2 antibodies, neutralizing and non-neutralizing, were mouse IgG1 clones bFM1 and bFM2, correspondingly, from Millipore (Billerica, MA, http://www.millipore.com); they were used at 0.2 μg/ml. Polyclonal goat anti-BMP4 and normal goat IgG control were used at 2 μg/ml, and recombinant human noggin was used at 30 ng/ml. These reagents, as well as mouse IgG1 isotype control, were from R&D Systems. For immunoprecipitation, the MSC-CM was incubated with either specific antibody (bFM1 or anti-BMP4) or control (mouse IgG1, goat IgG, or no antibody) at 5 μg/ml overnight at 4°C on a rotisserie shaker following by the addition of protein A/G-plus Agarose (Santa Cruz Biotechnology Inc., Santa Cruz, CA, http://www.scbt.com) for 1 hour. After beads were removed by centrifugation, supernatants were collected and sterilized by filtration.

For small interfering RNA (siRNA) transfection, MSCs were plated at 0.4×10^6 per six-well plate in αMEM/10% FBS. Next day cells were transfected with either ON-TARGETplus SMARTpool human BMP4 siRNA or control nontargeting pool at 25 nM, using DharmaFECT 1 (all reagents from Thermo Scientific Dharmacon, Lafayette, CO, http://www.thermoscientificbio.com) according to the manufacturer's instructions. The next day cells were harvested by trypsinization, washed with αMEM/10% FBS and then twice with Neurobasal medium, and plated in cocultures at 1.5×10^3 cells per cm^2 (their viability was >95%). After incubation for 5 days, cultures were lysed for gene expression quantification as described below.

Immunocytochemistry

Cultures grown on glass coverslips were fixed with 4% PFA for 20 minutes, washed once with PBS, and incubated in a blocking solution containing 10% normal donkey serum (Jackson Immunoresearch Laboratories, West Grove, PA, http://www.jacksonimmuno.com), 1% bovine serum albumin (Sigma-Aldrich), and 0.1% Triton X-100 for 30 minutes. Incubation with rat nestin-specific goat polyclonal antibody (1:1,000; R&D Systems) was performed overnight at 4°C. Other primary antibodies (rabbit polyclonal antibody against glial fibrillary acidic protein [GFAP] [1:2,000; Dako, Glostrup, Denmark, http://www.dako.com], mouse monoclonal antibody against microtubule-associated protein 2 [MAP2] [1:1,000; Sigma-Aldrich], or mouse monoclonal antibody against 2′,3′-cyclic nucleotide 3′-phosphodiesterase [CNP] [1:200; Millipore]) were added for 1 hour. After washing, coverslips were incubated for 1 hour with the corresponding secondary antibodies (suitable for multiple labeling, from Jackson Immunoresearch Laboratories): DyLight 488-conjugated AffiniPure donkey anti-goat $F(ab')_2$ fragments of IgG (1:1,000) with either DyLight 549-conjugated AffiniPure anti-rabbit $F(ab')_2$ fragments of IgG (1:2,000), or Cy3-conjugated AffiniPure donkey anti-mouse IgG (1:1,000). After washing, the slips were mounted with ProLong Gold antifade reagent containing 4′,6-diamidino-2-phenylindole (DAPI) (Invitrogen). In proliferation experiments, prior to fixation, cells were incubated for 7–8 hours with 10 μm of 5-bromo-2′-deoxyuridine (BRDU) (Sigma-Aldrich). Cultures then were fixed with 2% PFA, permeabilized with 0.5% Triton, and treated with DNase (MP Biomedicals) in the buffer containing 150 mM NaCl and 4.2 mM $MgCl_2$ for 1 hour at 37°C. The cultures were then postfixed with cold methanol for 10 minutes, blocked, and incubated with anti-BRDU monoclonal antibody (BD Pharmingen, San Jose, CA, http://www.bdbiosciences.com) and then with anti-mouse secondary antibody mentioned above, then with the TUJ1 antibody conjugated with Alexa Fluor (against neuronal class III β-tubulin) (Covance, Princeton, NJ, http://www.covance.com). Fluorescent microscopy was done using a Nikon Eclipse50i (Nikon, Melville, NY, http://www.nikon.com) and a Nikon DXM1200C digital camera. Under the conditions we used, none of the antibodies reacted with the human cells.

Gene Expression Quantification

The quantification of the mRNA expression of neural markers in adherent cultures was done in 96-well format. After culturing for indicated time, the culture medium was completely aspirated using a Nunc Immuno washer (Nalge Nunc International, Rochester, NY, http://www.nalgenunc.com) equipped with 10-μl pipette tips, and cells were lysed with either Cell-to-Signal (Ambion/Life Technologies, Pleasanton, CA, http://www.lifetechnologies.com) or SideStep lysis buffer (Agilent Technologies, Santa Clara, CA, http://www.agilent.com), 20 μl/well, for 3 minutes. Then the lysates were carefully pipetted up and down, and samples in quadruplicates were combined pairwise (thus making biological duplicates), transferred to a storage plate, and frozen at −80°C. For gene expression analysis, aliquots of lysates were diluted 1:10 with polymerase chain reaction (PCR)-grade water. In each experiment, all culture conditions were tested on the same PCR plate against the same standard curve for each neural marker. QuantiTect Probe RT-PCR Master Mix (Qiagen, Germantown, MD, http://www.qiagen.com) was used for one-step PCR with TaqMan gene expression assays (Applied Biosystems/Life Technologies). The species specificity of expression assays was established in preliminary experiments involving human MSCs and rat neural lysates, as well as purified RNA from rat and human brain. The following assays were used: rat-specific: nestin (Rn00564394_m1), MAP2 (Rn00565046_m1), GFAP (Rn00566603_m1), CNP (Rn01399463_m1), doublecortin (DCX) (Rn00584505_m1), and glyceraldehyde 3-phosphate dehydrogenase (rGAP) (Rn-1462661_g1); and human-specific: glyceraldehyde 3-phosphate dehydrogenase (huGAP) (4333764F), BMP4 (Hs00370078_m1), and FGF2 (Hs00266645_m1). A LightCycler 480 (Roche, Mannheim, Germany, http://www.roche.com) was programmed according to the Master Mix manufacturer's protocol, with 40–60 amplification cycles. The data were analyzed using the second derivative maximum method.

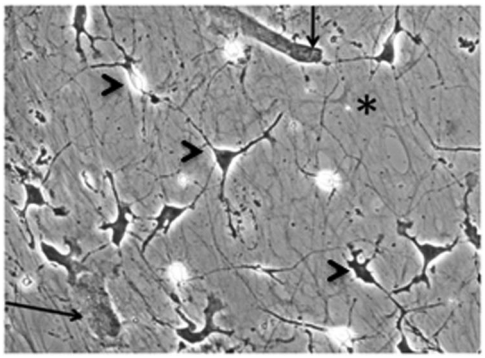

Figure 1. Coculture of rat cortical cells and human mesenchymal stromal cells (MSCs) on extracellular matrix (ECM), day 5. Note underlying ECM fibrils (asterisk), sparsely plated MSCs (arrows), and neural cells (distinct morphological types are indicated with arrowheads). The culture was paraformaldehyde-fixed, hematoxylin/eosin-stained, and microphotographed using phase contrast; magnification, ×200.

Neural Cell Proliferation in Cocultures

The proliferation of neural cells plated with or without MSCs (neural cells/MSCs, 10:1) was quantified by counting DAPI-stained nuclei on slides prepared for immunochemistry analysis as described above. Five microscopic fields at ×200 magnification were counted and averaged per condition, from two experiments. Very condensed or fragmented nuclei were considered dead. MSC nuclei excluded from counting based on their distinctive size.

RESULTS

Morphological and Immunocytochemical Characterization of Cocultures on ECM

Cortical cells and MSC cocultures grown on ECM were easily monitored microscopically during culturing, and the underlying ECM was visible until covered by cells. Figure 1 shows a typical coculture, fixed and stained on day 5. Neural cultures grown with or without MSCs were first analyzed using immunocytochemistry for rat nestin (Nes), a marker of neural stem cells/early progenitors, and MAP2, a neuronal marker (Fig. 2A). All cultures were also counterstained with nuclear dye DAPI (not shown). On day 1, single-positive green-stained Nes^+ and red-stained $MAP2^+$ cells were present in all tested cultures, along with some $MAP2^+Nes^+$ double-positive cells (stained yellow because of overlapping green and red). Nes^+, $MAP2^+$, and Nes^+MAP2^+ cell populations each made up approximately 30% of the total population, and double-negative cells (DAPI only, not shown) made up approximately 10%. Between days 3 and 7, no double-positive cells were detected, whereas both $MAP2^+$ and Nes^+ single-positive cells extended processes. The disappearance of double-positive Nes^+MAP2^+ cells after 2–3 days in culture could be explained by the maturation of Nes^+MAP2^+ neuronal precursors to young Nes^-MAP2^+ neurons. Nes^+ cells significantly increased in numbers forming colonies. In the presence of MSCs, the colonies appeared larger and more numerous. By day 9, however, there were striking numbers of $MAP2^+Nes^+$-double-positive (yellow-stained) cells appearing among abundant well-developed $MAP2^+$-only neurons and Nes^+-only cells, both in the absence and in the presence of MSCs. These $MAP2^+Nes^+$ cells could be clearly observed at later time points as well (supplemental online Fig. 1, day 12).

Double-staining of ECM-based cultures for astrocyte marker GFAP and nestin revealed the absence of GFAP reactivity before and on day 3 (Fig. 2B). Around day 5, red-stained $GFAP^+$ cells started appearing within colonies of green-stained Nes^+ cells in the presence, but not in the absence, of MSCs as single- or double-positive cells. Different colonies of Nes^+ cells had variable proportions of double-positive $GFAP^+Nes^+$ cells (yellow because of colocalization of red and green staining) and single-positive $GFAP^+$ cells (red). On day 9, all three phenotypes ($GFAP^+Nes^+$, $GFAP^-Nes^+$, and $GFAP^+Nes^-$) were present in all cultures, with $GFAP^+Nes^-$ predominating (details in supplemental online Fig. 2).

Oligodendrogenesis, assessed using the early oligodendrocyte marker CNP, was not detected before day 9. On day 12 (Fig. 2C), in the absence of MSCs, weak CNP reactivity was detected in only a very few, usually dividing cells. At the same time in cocultures, CNP^+ cells appeared in clusters, with CNP staining spreading to perinuclear area. CNP staining was never colocalized with Nes staining (not shown).

Cell Proliferation in Cocultures

Counting of non-MSC nuclei in DAPI-stained cultures on coverslips showed that in the presence of MSCs, rat neural cells tripled to quadrupled over the course of 7 days, whereas in the absence of MSCs, neural cells barely doubled (Fig. 3A), in agreement with our previous data [28]. According to the morphological appearance of DAPI-stained neural nuclei (Fig. 3B), 10%–20% of cells were dead at any given time.

By using BRDU incorporation on day 7, we also tested whether culturing on ECM with or without MSCs provided specifically for proliferation of neuronal precursors. Irrespective of MSC presence, cultures contained numbers of small cells with barely developed processes, which exhibited double reactivity with TUJ1 and anti-BRDU antibodies (Fig. 3C), indicating the presence of proliferating neuronal precursors. It was noted that the morphology of $BRDU^+TUJ1^+$ cells resembled the morphology of Nes^+MAP2^+ cells observed around days 7–9 (small cells with barely developed processes and bilobular nucleus) (supplemental online Fig. 1), which may imply that both these entities overlap.

The Dose Dependence and the Time Course of MSC-Induced Rat Neuropoiesis Quantified Using Quantitative Reverse Transcription-Polymerase Chain Reaction

To assess the MSC-dose dependence of neuropoiesis in cocultures, rat cortex cells were cultured in 96-well plates with increasing numbers of MSCs. Quantitative reverse transcription-polymerase chain reaction (qRT-PCR) assays for rat neural differentiation markers were used to quantify gene expression in cocultures on day 5 for Nes and CNP and on day 7 for all other genes. (These time points were chosen in preliminary experiments and justified as optimal on the basis of the data described below in this and subsequent sections.) A human-specific glyceraldehyde 3-phosphate dehydrogenase (GAP) assay was used to confirm the MSC presence on day 7. Figure 4A shows that total levels of Nes, CNP, MAP2, DCX, GFAP, and rat GAP expression in cocultures were directly dependent on the number of MSCs present. These effects were not caused by the amplification of human sequences, since MSCs cultured alone at the maximal

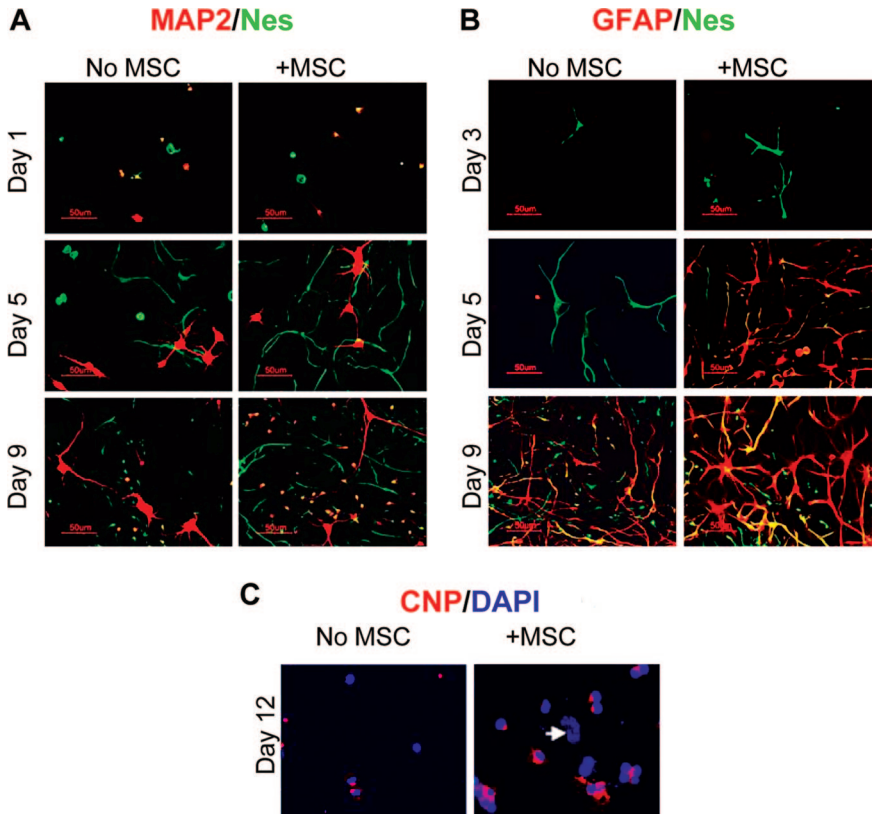

Figure 2. MSCs promote neural cell growth and differentiation on extracellular matrix; immunostaining. **(A):** MAP2 (red) and rat nestin (green). $MAP2^{+}Nes^{+}$ cells (yellow) were detected on days 1 and 9 but not on day 5. Magnification, ×200. **(B):** GFAP (red) and rat nestin (green); $GFAP^{+}Nes^{+}$ cells (yellow). Magnification, ×200. **(C):** CNP (red) and nuclei (blue) at day 12. Arrow indicates nucleus of an MSC. Magnification, ×400. Abbreviations: CNP, 2′,3′-cyclic nucleotide 3′-phosphodiesterase; DAPI, 4′,6-diamidino-2-phenylindole; GFAP, glial fibrillary acidic protein; MAP2, microtubule-associated protein 2; MSC, mesenchymal stromal cell; Nes, nestin.

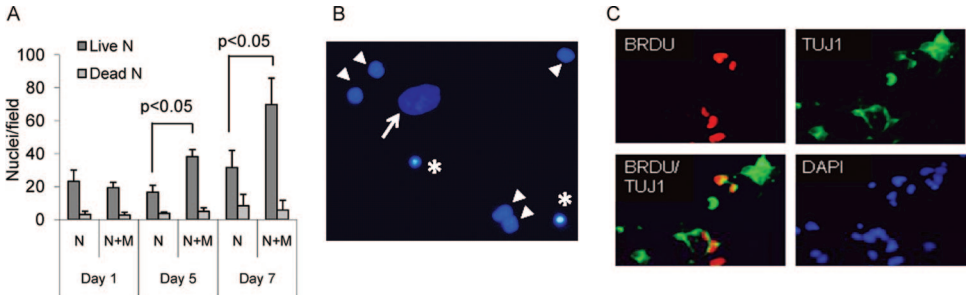

Figure 3. Mesenchymal stromal cells (MSCs) promote neural cell proliferation on extracellular matrix (ECM). Culturing on ECM supported proliferation of immature neurons. **(A):** Neural cell nuclei were counted in the presence and absence of MSCs. DAPI-stained paraformaldehyde-fixed cultures were assessed at a magnification of ×200. *p* values were calculated using the unpaired *t* test. **(B):** Illustration of morphological differences among DAPI-stained nuclei in a 7-day coculture allowing differential counting of nuclei: MSC nucleus (arrow), live neural cell nuclei (arrowheads), and dead (condensed) neural cell nuclei (asterisks). Magnification, ×400. **(C):** Cultures double-stained for BRDU and neuron-specific tubulin after a 7-hour incubation with BRDU on day 7. Magnification, ×200. The presence of $BRDU^{+}TUJ1^{+}$ cells indicated proliferation of neuronal precursors. Abbreviations: BRDU, 5-bromo-2′-deoxyuridine; DAPI, 4′,6-diamidino-2-phenylindole; M, mesenchymal stromal cells; N, neural cells; TUJ1, neuronal class III β-tubulin-specific antibody.

dose gave no signal in rat-specific reactions (not shown). Species specificity of assays for rat neural markers was further confirmed using purified RNA from human and rat brain: rat MAP2, DCX, CNP, and nestin assays produced no signal with human brain RNA, whereas the rat GFAP assay showed 10 times less efficient signal with human versus rat brain RNA (not shown).

The time course of total expression of rat neural markers in cultures on ECM was analyzed in the presence and in the absence of MSCs, 200 cells per well (Fig. 4B–4F). Samples collected and frozen at various time points were thawed and assayed all on the same day. Two hours after cell plating (day 0), only the neuronal markers (DCX and MAP2) (Fig. 4B, 4C) were detected in cultures at appreciable levels (threshold PCR cycles or crossing points [Cp] for DCX and MAP2 were 30 ± 1.2 and 33 ± 0.3, respectively), whereas nestin expression was very low ($Cp = 35 \pm 1.3$), and CNP and GFAP expression was below quantification ($Cp > 38$) and detection levels, correspondingly. Starting from the first day, nestin expression was constantly growing, being higher in the presence of MSCs than in their absence (Fig. 4D). CNP gene expression increased to quantification levels on day 4 in the

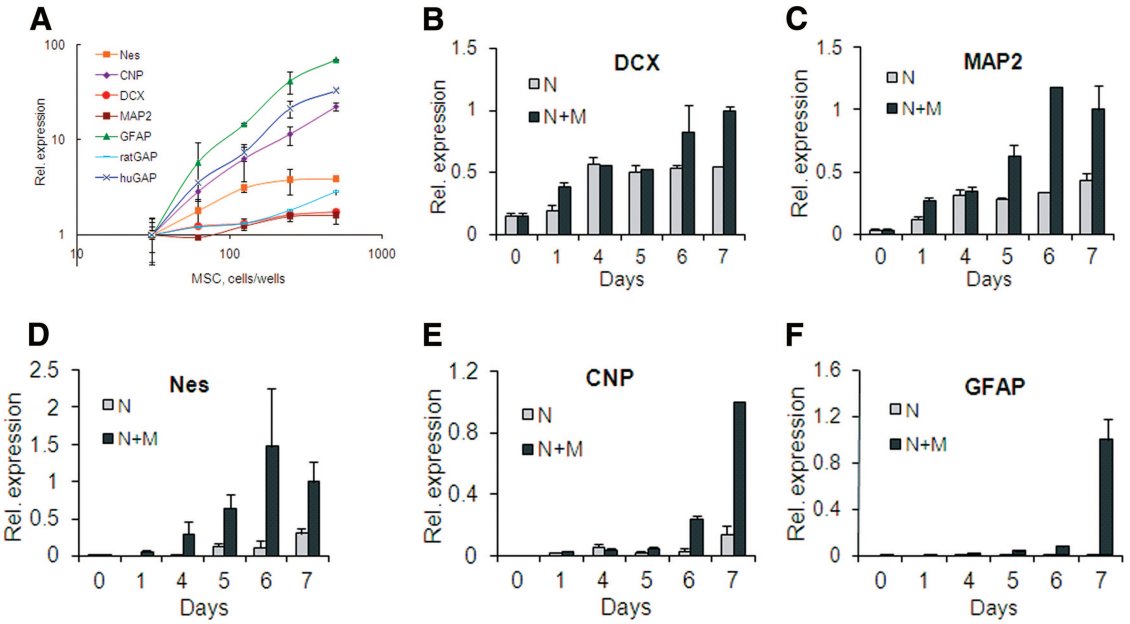

Figure 4. Time course and MSC-dose dependence of rat neural marker expression in cocultures; quantitative reverse transcription-polymerase chain reaction. **(A):** MSC-dose response. Expression levels in cocultures, with the lowest MSC dose set as 1. Nes and CNP expressions were tested on day 5, and MAP2, DCX, GFAP, GAPs, and human GAP expressions were tested on day 7. **(B–F):** Time course of neural marker expression in neural cells cultured alone or with MSCs. Expression levels in cocultures on day 7 were set as 1. **(B):** DCX. **(C):** MAP2. **(D):** Nes. **(E):** CNP. **(F):** GFAP. Abbreviations: CNP, 2′,3′-cyclic nucleotide 3′-phosphodiesterase; DCX, doublecortin; GFAP, glial fibrillary acidic protein; huGAP, human glyceraldehyde-3-phosphate dehydrogenase; M, mesenchymal stromal cells; MAP2, microtubule-associated protein 2; MSC, mesenchymal stromal cell; N, neural cells; Nes, nestin; ratGAP, rat glyceraldehyde-3-phosphate dehydrogenase; Rel., relative.

presence of MSCs and on day 6 in their absence (Fig. 4E). GFAP expression was practically absent during all 7-day culturing without MSCs; in cocultures, however, it could be detected on days 4–5, rising sharply by day 7 (Fig. 4F). DCX and MAP2 (Fig. 4B, 4C) were highly expressed both in the presence and in the absence of MSCs. However, typically at an early time point (day 1) and around days 6–7, expression of neuronal markers was significantly ($p < .05$) higher in cocultures compared with their expression in neural cells alone, preceding or coinciding with extensive neuritogenesis (day 1) and the formation of de novo neurons (around days 6–7) (Fig. 3B), suggesting that the presence of MSCs stimulated these events. On the basis of data presented on Figure 4B–4F, the optimal timing for the detection of nestin and CNP expression was determined to be day 5 (regarding the timing of CNP, see also next section) and for GFAP, DCX, and MAP2 it was day 7.

We also tested the effects of cell substrates on MSC-induced neuropoiesis by comparing neural marker induction in cocultures grown on either ECM or Orn/Fn or in the absence of attachment substrate in ULA wells (supplemental online Fig. 3). Cocultures on ECM, but not on Orn/Fn, exhibited nestin expression levels similar to those in FGF2/EGF-driven neurospheres; on ECM, there were also the highest levels of GFAP. Thus, ECM-based cocultures contained the most diverse neural cell population.

Inhibition of CNP Expression at Higher Doses of MSCs

Although on day 5 CNP expression levels in cocultures were directly dependent on MSC dose, at later time points higher doses of MSCs progressively inhibited a CNP expression increase, exhibiting a biphasic dose-response curve (Fig. 5A). This was confirmed at the protein level on day 12 by immunocytochemistry.

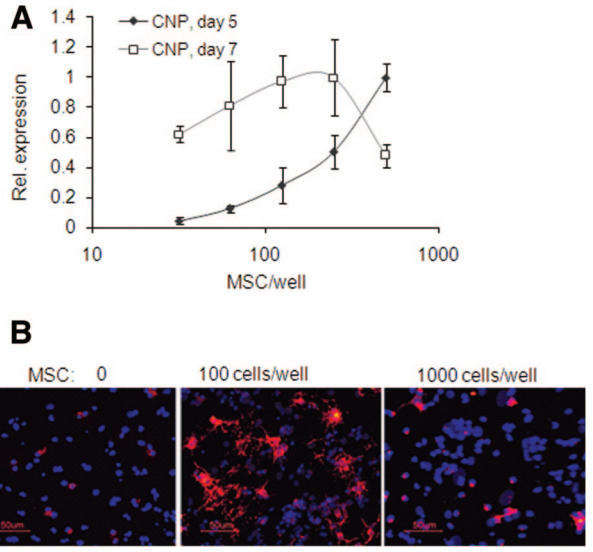

Figure 5. The biphasic effect of MSC dose on expression of rat CNP in cocultures. **(A):** The CNP gene expression assessed using quantitative reverse transcription-polymerase chain reaction was directly dependent on MSC dose on day 5 but was inhibited by higher MSC doses on day 7. Values are expressed relative to the highest level on each day. **(B):** MSCs promoted CNP protein expression; however, lower MSC doses promoted more advanced oligodendrocyte differentiation on day 12 than did higher doses. Magnification, ×200. Abbreviations: CNP, 2′,3′-cyclic nucleotide 3′-phosphodiesterase; MSC, mesenchymal stromal cell; Rel., relative.

Both doses of MSCs, 1,000 and 100 cells per cm^2, induced CNP protein; however, the 1,000 cells per cm^2 dose of MSCs induced less CNP staining than did the 100 cells per cm^2 dose of MSCs (Fig. 5B).

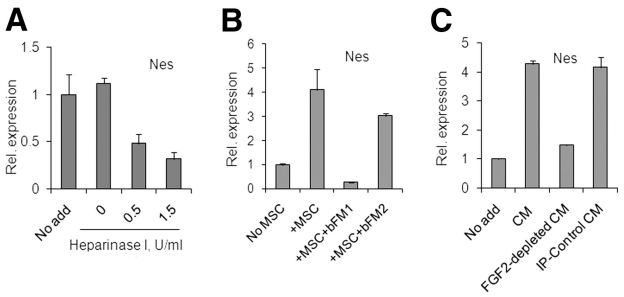

Figure 6. MSC-derived FGF2 mediates the MSC-driven nestin increase in cocultures; quantitative reverse transcription-polymerase chain reaction. **(A):** Heparinase I pretreatment of extracellular matrix-coated wells reduced basal levels of Nes in neural cultures. **(B):** Neural cells and MSCs, 200 cells per well, were cocultured in the presence or absence of isotype-matching anti-FGF2 antibodies, either bFM1 (neutralizing) or bFM2 (non-neutralizing). **(C):** Neural cells were cultured in the presence or absence of 40% MSC-CM, either intact, FGF2-immunodepleted, or control-treated. Abbreviations: CM, mesenchymal stromal cell-conditioned medium; FGF2, fibroblast growth factor 2; IP, immunoprecipitation; MSC, mesenchymal stromal cell; Nes, nestin; Rel., relative.

The Neutralization of FGF2 Abolishes MSC-Induced Rat Nestin Increases in Cocultures

A pretreatment of ECM with Heparinase 1 prior to the neural cell plating resulted in dose-dependent decrease of nestin expression in cortical cells (Fig. 6A), indicating that heparan sulfate proteoglycans (HSPGs) in ECM contributed to the effective support of Nes^{+} neural cell growth, possibly by participating in FGF2 signaling. MSC preparations expressed FGF2: by qRT-PCR, averaged $Cp = 28 \pm 0.6$ in samples from four donors (for human GAP, $Cp = 22 \pm 0.4$). To inhibit secreted FGF2, the FGF2-neutralizing antibody with both anti-human and anti-rat reactivity, bFM1, was used. In cocultures, bFM1 downregulated nestin below the background levels, whereas the control isotype-matching FGF2-specific antibody lacking FGF2-neutralizing activity, bFM2, showed no significant inhibition (Fig. 6B). An FGF2-immunodepleted MSC-CM induced no significant increase of nestin expression, whereas intact MSC-CM or MSC-CM treated with a control irrelevant antibody induced nestin expression (Fig. 6C). These results strongly suggested that MSC-derived FGF2 was the main factor responsible for nestin induction in cocultures and in the MSC-CM. These results also indicated that the basal nestin expression in cortical cells grown on ECM in the absence of MSCs was dependent on FGF2, either of rat or human origin.

MSC-Derived BMP4 Is One of the BMPs Responsible for Astrogenic Effects of MSCs, and Active BMP4 Is Poorly Diffusible

Induction of rat GFAP stimulated by MSCs was generally stronger than that stimulated by MSC-CM; this contrasted to the induction of rat nestin, which was efficiently upregulated by either MSCs or MSC-CM. For example, similar levels of nestin were induced by either 200 cells per well of MSCs or 10% MSC-CM; however, in the same experiment GFAP expression induced by MSC-CM was significantly lower than that induced by cells (Fig. 7A). This suggested that astrogenic activity was underrepresented in MSC-CM, as compared with the astrogenic activity exhibited in coculture setting.

We tested the effects of BMP inhibition on MSC-driven GFAP induction. Various BMPs were expressed in MSC preparations:

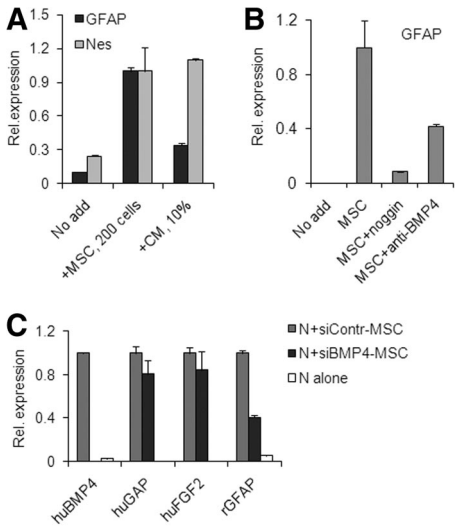

Figure 7. Bone morphogenetic proteins, and particularly BMP4, mediate MSC-driven induction of rat GFAP expression in cocultures; quantitative reverse transcription-polymerase chain reaction. **(A):** Both nestin and GFAP were strongly induced by MSCs, whereas MSC-CM mediated weak induction of GFAP and strong induction of nestin. **(B):** Recombinant noggin or human BMP4-specific neutralizing antibody inhibited GFAP increase. **(C):** Silencing of BMP4 in MSCs decreased GFAP induction in cocultures. MSCs transfected with either BMP4- or control-siRNA were cocultured with neural cells for 5 days followed by gene expression analysis. Expression levels are shown relative to levels in control cocultures, which are set as 1. In cocultures with BMP4-siRNA transfectants, human BMP4 expression was knocked down and rat GFAP expression was lowered, whereas human FGF2 and human GAP expression were unchanged, compared with control. Abbreviations: BMP4, bone morphogenetic protein; CM, mesenchymal stromal cell-conditioned medium; GFAP, glial fibrillary acidic protein; huBMP4, human bone morphogenetic protein 4; huFGF2, human fibroblast growth factor 2; huGAP, human glyceraldehyde-3-phosphate dehydrogenase; MSC, mesenchymal stromal cell; N, neural cells; Nes, nestin; Rel., relative; rGFAP, rat glial fibrillary acidic protein; siBMP4-MSC, mesenchymal stromal cells transfected with bone morphogenetic protein 4-targeted small interfering RNA; siContr-MSC, mesenchymal stromal cells transfected with negative control small interfering RNA.

averaged crossing points in qRT-PCR analyses (four donors) for BMP2, BMP4, and BMP6 were 36 ± 0.3, 31 ± 1.0, and 33 ± 0.6, respectively. Recombinant noggin, a BMP antagonist, very efficiently inhibited GFAP induction in cocultures, whereas a neutralizing human BMP4-specific antibody had a significant but partial effect (Fig. 7B). This strongly suggested that several BMPs, including BMP4, were driving astrogenesis in cocultures. Attempts to deplete GFAP-inducing activity from MSC-CM by BMP4 immunoprecipitation were not successful, although the same antibody effectively blocked GFAP induction driven by recombinant BMP4 in control experiments (not shown).

The lower astrogenic activity of MSC-CM, as compared with MSCs, the lack of an inhibitory effect of BMP4 immunodepletion from MSC-CM, but some inhibitory effect of BMP4 neutralization in cocultures—all suggest that either the active BMP4 resides within the cell-ECM compartment, rather than in the MSC-CM, or that it is produced by rat cells. To test whether active BMP4 in cocultures was produced by MSCs, BMP4-siRNA, or control-siRNA were transfected into MSCs prior to coculturing. The day after transfection, equal cell

numbers of transfectants were plated with rat cortical cells and cocultured for 5 days. On day 5, expression of human BMP4 was virtually undetectable in cocultures with BMP4-siRNA transfectants but not with control transfectants, whereas expression of human GAP and FGF2 was not significantly different between these cocultures (Fig. 7C). Rat GFAP was significantly reduced in cocultures with BMP4-siRNA but not with control transfectants. This strongly suggested that in ECM-based cocultures, BMP4 was one of the BMPs responsible for astrogenesis, that it was produced by MSCs, and that active BMP4 stayed within cell-ECM compartment rather than being released into the medium.

Discussion

Here we have characterized a system that enables the quantitative analysis of neuropoietic activity of MSCs in direct cross-species cocultures. The system has the following key features: (a) mesenchymal cell-derived ECM as substrate; (b) the same microenvironment from start to finish; (c) no external growth factors; (d) both MSC-secreted diffusible and matricellular factors can be evaluated; and (e) microplate format, low cell plating density, and qRT-PCR-based readout using total lysates provide high sensitivity and versatility.

Previously, we have shown that human MSC-derived ECM and, to a greater extent, SB623 cell-derived ECM, permit the growth and differentiation of rat embryonic cortical cells at relatively low cell plating densities and in the absence of growth factors [28]. Here we have demonstrated that ECM created a favorable environment for Nes^+ cells (Fig. 2; supplemental online Fig. 2) and that ECM's integral HSPGs were essential (Fig. 6A). The crucial role of HSPG and the below-basal level decrease of Nes expression upon FGF2-neutralizing antibody (Fig. 6B) suggested the important role of FGF2 in ECM-based cultures even in the absence of MSCs. This FGF2 (of rat origin, human origin, or both) seems to provide a physiological support for survival and the slow proliferation of neural stem/precursor cells. Recent reports identified mesenchymal cell-derived ECM as an integral part of an in vivo neural stem cell niche in the form of extravascular basal laminae (fractones), and its HSPGs were implicated in the accumulation of FGF2 [31, 32]. Thus, neural cell culturing on a mesenchymal ECM substrate could model the in vivo environment in stem cell niche. Although we optimized our system using SB623-cell-derived ECM, an MSC-ECM-based system can produce similar results (not shown) but will require longer culturing times and likely other adjustments. Specific properties of SB623-derived ECM that make it a better substrate for neural growth are being studied.

The presence of MSCs dose-dependently increased growth and differentiation of neural cells (Figs. 2–4), and effects of as few as 50 human MSCs per 5,000 rat neural cells could be detected using qRT-PCR analysis of rat neural marker expression (Fig. 4A). Measured expression levels reflected a cumulative outcome of several processes in cocultures. For example, an MSC-driven increase in total nestin expression (Fig. 4D) was a result of increased expression of nestin per cell and of grown numbers of both Nes^+-stem cells and double-positive immature precursors (Fig. 2A). MSC-driven increases in MAP2 or DCX expression (Fig. 4B, 4C) likely reflected MSC-enhanced neuritogenesis at day 1 (Fig. 2A) [15, 22, 33, 34], and possibly an MSC-expedited appearance of de novo neurons ($MAP2^+Nes^+$ and $BRDU^+TUJ1^+$) around day 6 or later (Figs. 2A, 3C). These results are in agreement with previous reports, which demonstrated the stimulating effects of MSCs on proliferation of neural precursors of neurosphere origin and on neuronal differentiation [23–25].

MSCs are known to secrete many neurotrophic factors (reviewed in [35]), and the secretion of some of them, including BMP4, FGF2, EGF, vascular endothelial growth factor, and platelet-derived growth factor-AA, has been confirmed in some MSC batches used here [30]. Experiments with an FGF2-neutralizing antibody demonstrated that MSC-produced FGF2 was the major factor responsible for the MSC-driven nestin induction on ECM, both in cocultures and in the presence of MSC-CM (Fig. 6B, 6C). The crucial role of FGF2 in the maintenance of neural stem cells is well known [36, 37]; our results showed that in the presence of ECM, the effects of MSC-derived FGF2 on rat nestin overwhelmed other possible contributors.

Astrogenesis evident from GFAP expression was a hallmark of serum-free ECM-based neural cultures. Efficient Nes^+ cell spreading observed on ECM was likely its prerequisite [38]. MSCs greatly promoted GFAP expression (Figs. 2B, 4F). BMPs, and particularly BMP4, which is abundantly expressed in MSCs ([39] and our results), seemed to be major mediators of this effect, since noggin, an inhibitor of BMP activity, reduced GFAP induction by ~90%, and BMP4-neutralizing antibody had a partial inhibitory effect in cocultures (Fig. 7B). BMP4 was previously implicated in mediating astrogenic effects of specially induced rat MSCs in cocultures with mouse neurospheres [40]. We observed that MSC-CM was less astrogenic than MSCs (Fig. 7A, in agreement with [25]) and that the residual astrogenic activity of MSC-CM could not be removed by immunodepleting BMP4. At the same time, MSCs with BMP4 silenced using siRNA showed reduced astrogenic activity (Fig. 7C). Taken together, these results suggested that astrogenic activity of MSCs was mediated in part by BMPs, and specifically, by human BMP4, and that the active BMP4 was associated with cells/ECM, rather than being released to MSC-CM. These results do not exclude the possibility that MSCs can induce some secretion of rat BMPs [41] or that other MSC factors, such as transforming growth factor-β (TGFβ), were involved [25, 42], although we were unable to inhibit astrogenesis in cocultures by blocking TGFβ1 (not shown).

Oligodendrocytic differentiation was monitored using an early oligodendrocytic marker, the myelin-processing enzyme CNP, whose expression grows throughout the maturation process [43]. In agreement with previous reports [24, 44, 45], oligodendrogenesis in our cocultures was MSC-dependent; however, only at earlier time points was there a direct MSC-dose dependence; later, higher doses of MSCs inhibited the growth of CNP, so that a dose-dependence curve became reversed, which was demonstrated on both mRNA and protein levels (Fig. 5). This can be explained by a previously described negative feedback mechanism, when cell-to-cell contact between oligodendrocyte precursors controls their own expansion and differentiation [46, 47]. Indeed, we observed the same biphasic dose response to high doses of MSC-CM (not shown), which indicated that the inhibition was not due to contacts with mesenchymal cells.

Conclusion

We characterized here an in vitro system that enables the quantitative multifactorial analysis of MSC effects on a primary neural cell population. The system preserves the complexity and some of the intrinsic interactions of primary neural cell population. By implicating MSC-derived FGF2 and BMP4 in enhancement of neuropoiesis, we demonstrated that the system can be used to elucidate both soluble and matricellular factors. Finally, the system can be used for comparing the potencies of various lots of MSCs or their derivatives, as well as for studying the effects of neural population on MSCs.

Author Contributions

I.A.: conception and design, collection and/or assembly of data, data analysis and interpretation, manuscript writing; M.M.: provision of study material; C.C.C.: conception and design, manuscript writing, final approval of manuscript

Disclosure of Potential Conflicts of Interest

I.A., M.M., and C.C.C. are employees of SanBio, Inc., and have compensated employment, intellectual property, and stock options.

References

1 Torrente Y, Polli E. Mesenchymal stem cell transplantation for neurodegenerative diseases. Cell Transplant 2008;17:1103–1113.

2 Qu C, Mahmood A, Lu D et al. Treatment of traumatic brain injury in mice with marrow stromal cells. Brain Res 2008;1208:234–239.

3 Hofstetter CP, Schwarz EJ, Hess D et al. Marrow stromal cells form guiding strands in the injured spinal cord and promote recovery. Proc Natl Acad Sci USA 2002;99:2199–2204.

4 Li Y, Chen J, Wang L et al. Intracerebral transplantation of bone marrow stromal cells in a 1-methyl-4-phenyl-1,2,3,6-tetrahydropyridine mouse model of Parkinson's disease. Neurosci Lett 2001;316:67–70.

5 Li Y, Chen J, Zhang CL et al. Gliosis and brain remodeling after treatment of stroke in rats with marrow stromal cells. Glia 2005;49:407–417.

6 Chopp M, Zhang XH, Li Y et al. Spinal cord injury in rat: Treatment with bone marrow stromal cell transplantation. Neuroreport 2000;11:3001–3005.

7 Glavaski-Joksimovic A, Virag T, Chang QA et al. Reversal of dopaminergic degeneration in a parkinsonian rat following micrografting of human bone marrow-derived neural progenitors. Cell Transplant 2009;18:801–814.

8 van Velthoven CT, Kavelaars A, van Bel F et al. Repeated mesenchymal stem cell treatment after neonatal hypoxia-ischemia has distinct effects on formation and maturation of new neurons and oligodendrocytes leading to restoration of damage, corticospinal motor tract activity, and sensorimotor function. J Neurosci 2010;30:9603–9611.

9 Cova L, Armentero MT, Zennaro E et al. Multiple neurogenic and neurorescue effects of human mesenchymal stem cell after transplantation in an experimental model of Parkinson's disease. Brain Res 2010;1311:12–27.

10 Yoo SW, Kim SS, Lee SY et al. Mesenchymal stem cells promote proliferation of endogenous neural stem cells and survival of newborn cells in a rat stroke model. Exp Mol Med 2008;40:387–397.

11 Tfilin M, Sudai E, Merenlender A et al. Mesenchymal stem cells increase hippocampal neurogenesis and counteract depressive-like behavior. Mol Psychiatry 2010;15:1164–1175.

12 Munoz JR, Stoutenger BR, Robinson AP et al. Human stem/progenitor cells from bone marrow promote neurogenesis of endogenous neural stem cells in the hippocampus of mice. Proc Natl Acad Sci USA 2005;102:18171–18176.

13 Kan I, Barhum Y, Melamed E et al. Mesenchymal stem cells stimulate endogenous neurogenesis in the subventricular zone of adult mice. Stem Cell Rev 2011;7:404–412.

14 Walker PA, Harting MT, Jimenez F et al. Direct intrathecal implantation of mesenchymal stromal cells leads to enhanced neuroprotection via an NFkappaB-mediated increase in interleukin-6 production. Stem Cells Dev 2010;19:867–876.

15 Crigler L, Robey RC, Asawachaicharn A et al. Human mesenchymal stem cell populations express a variety of neuro-regulatory molecules and promote neuronal cell survival and neuritogenesis. Exp Neurol 2006;198:54–64.

16 Caplan AI, Dennis JE. Mesenchymal stem cells as trophic mediators. J Cell Biochem 2006;98:1076–1084.

17 Hawryluk GW, Mothe AJ, Chamankhah M et al. In vitro characterization of trophic factor expression in neural precursor cells. Stem Cells Dev 2012;21:432–447.

18 Nicaise C, Mitrecic D, Pochet R. Brain and spinal cord affected by amyotrophic lateral sclerosis induce differential growth factors expression in rat mesenchymal and neural stem cells. Neuropathol Appl Neurobiol 2011;37:179–188.

19 Mondal D, Pradhan L, LaRussa VF. Signal transduction pathways involved in the lineage-differentiation of NSCs: Can the knowledge gained from blood be used in the brain? Cancer Invest 2004;22:925–943.

20 Garwood J, Rigato F, Heck N et al. Tenascin glycoproteins and the complementary ligand DSD-1-PG/ phosphacan: Structuring the neural extracellular matrix during development and repair. Restor Neurol Neurosci 2001;19:51–64.

21 Kinnunen A, Niemi M, Kinnunen T et al. Heparan sulphate and HB-GAM (heparin-binding growth-associated molecule) in the development of the thalamocortical pathway of rat brain. Eur J Neurosci 1999;11:491–502.

22 Lou S, Gu P, Chen F et al. The effect of bone marrow stromal cells on neuronal differentiation of mesencephalic neural stem cells in Sprague-Dawley rats. Brain Res 2003;968:114–121.

23 Kang SK, Jun ES, Bae YC et al. Interactions between human adipose stromal cells and mouse neural stem cells in vitro. Brain Res Dev Brain Res 2003;145:141–149.

24 Bai L, Caplan A, Lennon D et al. Human mesenchymal stem cells signals regulate neural stem cell fate. Neurochem Res 2007;32:353–362.

25 Robinson AP, Foraker JE, Ylostalo J et al. Human stem/progenitor cells from bone marrow enhance glial differentiation of rat neural stem cells: A role for transforming growth factor β and notch signaling. Stem Cells Dev 2011;20:289–300.

26 Campos LS. Neurospheres: Insights into neural stem cell biology. J Neurosci Res 2004;78:761–769.

27 Hack MA, Sugimori M, Lundberg C et al. Regionalization and fate specification in neurospheres: The role of Olig2 and Pax6. Mol Cell Neurosci 2004;25:664–678.

28 Aizman I, Tate CC, McGrogan M et al. Extracellular matrix produced by bone marrow stromal cells and by their derivative, SB623 cells, supports neural cell growth. J Neurosci Res 2009;87:3198–3206.

29 Dao MA, Tate CC, Aizman I et al. Comparing the immunosuppressive potency of naive marrow stromal cells and Notch-transfected marrow stromal cells. J Neuroinflammation 2011;8:133.

30 Tate CC, Fonck C, McGrogan M et al. Human mesenchymal stromal cells and their derivative, SB623 cells, rescue neural cells via trophic support following in vitro ischemia. Cell Transplant 2010;19:973–984.

31 Mercier F, Kitasako JT, Hatton GI. Anatomy of the brain neurogenic zones revisited: Fractones and the fibroblast/macrophage network. J Comp Neurol 2002;451:170–188.

32 Kerever A, Schnack J, Vellinga D et al. Novel extracellular matrix structures in the neural stem cell niche capture the neurogenic factor fibroblast growth factor 2 from the extracellular milieu. Stem Cells 2007;25:2146–2157.

33 Führmann T, Montzka K, Hillen LM et al. Axon growth-promoting properties of human bone marrow mesenchymal stromal cells. Neurosci Lett 2010;474:37–41.

34 Kamei N, Tanaka N, Oishi Y et al. Bone marrow stromal cells promoting corticospinal axon growth through the release of humoral factors in organotypic cocultures in neonatal rats. J Neurosurg Spine 2007;6:412–419.

35 Maltman DJ, Hardy SA, Przyborski SA. Role of mesenchymal stem cells in neurogenesis and nervous system repair. Neurochem Int 2011;59:347–356.

36 Temple S, Qian X. Neuron. bFGF, neurotrophins, and the control or cortical neurogenesis. Neuron 1995;15:249–252.

37 Mudò G, Bonomo A, Di Liberto V et al. The FGF-2/FGFRs neurotrophic system promotes neurogenesis in the adult brain. J Neural Transm 2009;116:995–1005.

38 Goetschy JF, Ulrich G, Aunis D et al. Fibronectin and collagens modulate the proliferation and morphology of astroglial cells in culture. Int J Dev Neurosci 1987;5:63–70.

39 Seib FP, Franke M, Jing D et al. Endogenous bone morphogenetic proteins in human bone marrow-derived multipotent mesenchymal stromal cells. Eur J Cell Biol 2009;88:257-271.

40 Wislet-Gendebien S, Bruyère F, Hans G et al. Nestin-positive mesenchymal stem cells favour the astroglial lineage in neural progenitors and stem cells by releasing active BMP4. BMC Neurosci 2004;5:33–44.

41 Xin H, Li Y, Chen X et al. Bone marrow stromal cells induce BMP2/4 production in oxygen-glucose-deprived astrocytes, which promotes an astrocytic phenotype in adult subventricular progenitor cells. J Neurosci Res 2006;83:1485–1493.

42 Stipursky J, Gomes FC. TGF-beta1/SMAD signaling induces astrocyte fate commitment in vitro: Implications for radial glia development. Glia 2007;55:1023–1033.

43 Pfeiffer SE, Warrington AE, Bansal R. The oligodendrocyte and its many cellular processes. Trends Cell Biol 1993;3:191–197.

44 Steffenhagen C, Dechant FX, Oberbauer E et al. Mesenchymal stem cells prime proliferating adult neural progenitors toward an oligodendrocyte fate. Stem Cells Dev 2012;21: 1838–1851.

45 Rivera FJ, Kandasamy M, Couillard-Despres S et al. Oligodendrogenesis of adult neural progenitors: Differential effects of ciliary neurotrophic factor and mesenchymal stem cell derived factors. J Neurochem 2008;107:832–843.

46 Hugnot JP, Mellodew K, Pilcher H et al. Direct cell-cell interactions control apoptosis and oligodendrocyte marker expression of neuroepithelial cells. J Neurosci Res 2001;65:195–207.

47 Zhang H, Miller RH. Density-dependent feedback inhibition of oligodendrocyte precursor expansion. J Neurosci 1996;16:6886–6895.

See www.StemCellsTM.com for supporting information available online.